An introduction to visibility modeling

Jean Philippe Berger, Damien Segransan [a,b]

[a] *Laboratoire d'Astrophysique de Grenoble, Observatoire de Grenoble BP 53 F-38041 GRENOBLE Cédex 9, France*

[b] *Observatoire de Geneve*

Abstract

In order to exploit current interferometers the observer needs to be familiar with the process of visibility modeling. We introduce the tools that are required to allow the construction of a proper visibility model. We start with the description of the essential visibility analytical building blocks and then show how to arrange them together in order to construct a more complex picture. As an example we construct an analytical model of the visibility curve expected from an accretion disk model. Finally we discuss few issues an observer should be aware of when modelling visibilities.

Key words:

1 Introduction

Today, images are routinely produced by radio-interferometers such as the VLA or IRAM. Yet, this is not the case in the optical domain (infrared-visible wavelengths) where image reconstruction from a long baseline interferometer is still a celebrated achievement [1]. Astronomers should therefore be prepared to deal with visibility curves rather than true images. This should not prevent them from carrying out excellent scientific observations.

The purpose of this paper is to get the reader familiar with interpreting visibility data by describing visibility signatures of the most common morphologies. In Section 2 we recall the relation between object and visibility and introduce the most useful morphologies: the "building blocks" of modeling. In section 3 we describe how to compose the previous elementary functions in order to

[1] Hopefully with the second generation VLTI instruments this will soon not be the case.

build a more complex model. Actual examples extracted from the litterature are finally presented in section 4.

It is beyond the scope of this paper to describe all the mathematical derivations, most of which are straightforward. The process of model fitting by itself is described in Eric Thibaut's contribution.

2 The interferometric visibility

2.1 Assumptions

The van Cittert- Zernike theorem (see C. Haniff, same volume) expresses the link between brightness distribution I of the object and the corresponding complex visibility ν. It is a Fourier transform.

$$I(\alpha,\beta) = \int_{-\infty}^{\infty}\int_{-\infty}^{\infty} \nu(u,v)\exp(2\pi i(\alpha u+\beta u))dudv \qquad (1)$$

where (α,β) represents angular coordinates on the sky (units of radians) and (u,v) are the coordinates describing the spatial frequencies of the brightness distribution. We can relate u and v to the baseline vector $\vec{B}$: $u = B_u/\lambda, v = B_v/\lambda$ where λ is the wavelength and B_u and B_v are the projection of the baseline vector on the two axes. Units for u and v are often expressed in fringe cycles per radian. The left part of Figure 1 illustrates these choices. Let us call $\vec{s}$ the vector arising from the center of the baseline and pointing towards the source; this defines the origin of the object coordinates. The reader interested in the orientation conventions should read D. Segransan's contribution in this volume.

The following discussions will be restricted to the pure monochromatic case. Reconstructing the brightness distribution from the complex visibilities is often not as simple as inverting visibility in Equation 1; a sampling function $S(u,v)$ that expresses the sparse (u,v) coverage has to be introduced as a multiplicating factor. The Fourier inversion no longer leads to the true brightness distribution but rather to the brightness distribution convolved with the "dirty" beam. Further numerical deconvolutions are required. Here we will restrict ourselves to the perfect and impossible case of continuous sampling, were the relation between visibility and brightness distribution is a pure Fourier transform.

Lastly, the complex visibility $\nu(u,v)$ is not normalized. It contains a scaling factor that is directly proportional to the intensity of the source. Here we will

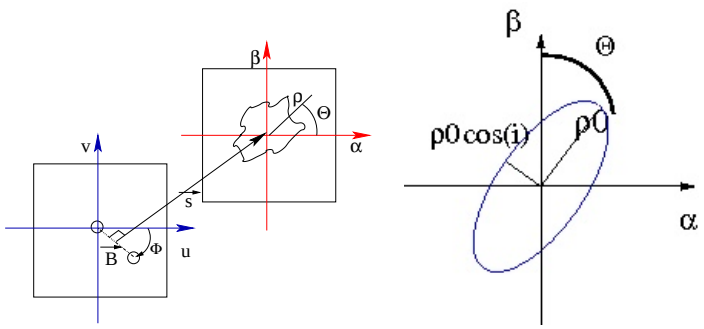

Fig. 1. Left: notations used in this chapter to describe the interferometer plane and the object brightness distribution plane. Right: thin ellipse in the object plane. ρ_0 and $\rho_0 \cos(i)$ are semi-major and semi-minor axis and Θ the inclination with respect to the β axis (the position angle).

restrict the discussion to the normalized visibility V:

$$V(u,v) = \frac{\nu(u,v)}{\nu(0,0)} \tag{2}$$

One should keep in mind that the squared visibility is often the actual quantity measured by interferometers.

2.2 Fourier transform

It is useful, before starting, to recall some basic properties of the Fourier transform which links brightness distribution and complex visibility.

$$\text{Addition :} \quad \text{FT}\{I_1(\alpha,\beta) + I_2(\alpha,\beta)\} = \nu_1(u,v) + \nu_2(u,v) \tag{3}$$

$$\text{Similarity :} \quad \text{FT}\{I(a\alpha, b\beta)\} = \frac{1}{|ab|}\nu(u/a, v/b) \tag{4}$$

$$\text{Translation :} \quad \text{FT}\{I(\alpha-\alpha_0, \beta-\beta_0)\} = \nu(u,v)\exp[2\pi i(u\alpha_0 + v\beta_0)] \tag{5}$$

$$\text{Convolution :} \quad \text{FT}\{I_1(\alpha,\beta) \times I_2(\alpha,\beta)\} = \nu_1(u,v).\nu_2(u,v) \tag{6}$$

2.3 Visibility curve for a circularly symmetric object.

When the object has circular symmetry it is easier to switch to polar coordinates. The object brightness distribution being even and real, the cor-

responding visibility will consequently be even. We define $\rho = \sqrt{\alpha^2 + \beta^2}$ and $\Theta = \text{atan}\frac{\alpha}{\beta}$ as the polar coordinates in the object plane. We define $r = \sqrt{u^2 + v^2}, \phi = \text{atan}\frac{\text{v}}{\text{u}}$ are the polar coordinates in the (u,v) plane.

The expression for the visibility in polar coordinates can be extracted directly from the inversion of relation inverse of Equation 1, it is:

$$\nu(r, \phi) = \int_0^{2\pi} \int_0^{\infty} I(\rho, \Theta) \exp(-2\pi i(\rho r \cos(\Theta - \phi)))\rho d\rho d\Theta \tag{7}$$

Because of the symmetry $I(\rho, \Theta) = I(\rho)$ and $\nu(r, \phi) = \nu(\rho)$. Simplifying the cosine expression the previous equation becomes:

$$\nu(r) = \int_0^{2\pi} \int_0^{\infty} I(\rho) \exp(-2\pi i \rho r \cos\Theta)\rho d\rho d\Theta \tag{8}$$

Introducing the zeroth-order Bessel function of the first kind allows the computation of the integral with respect to Θ:

$$J_0(x) = \frac{1}{2\pi} \int_0^{2\pi} \exp(-ixcos\Theta)d\Theta \tag{9}$$

which leads to the final expression for the visibility:

$$\nu(r) = 2\pi \int_0^{\infty} I(\rho) J_0(2\pi\rho r)\rho d\rho \tag{10}$$

The link between ν and I is now a Hankel transform. This expressions allows us to compute visibility curves for a wide variety of distributions using the many relations linking Bessel functions (recurrence relations, distribution expressions etc...)

Another way of looking at Equation 10 is to consider the brightness distribution of a circular ring of infinitesimally thickness (radius ρ_0), which can be represented by the following brightness:

$$I(\rho) = \frac{1}{2\pi\rho_0}\delta(\rho - \rho_0) \tag{11}$$

the corresponding normalized visibility is then:

$$V(u, v) = J_0(2\pi\rho_0 r) \tag{12}$$

Model	Intensity distribution	Visibility	Comment
Point	$I(\alpha,\beta)=\delta(\alpha-\alpha_0,\beta-\beta_0)$ (13)	$V(u,v)=\exp^{-2\pi i(u\alpha_0+v\beta_0)}$ (14)	Simulates an unresolved point source.
Gaussian disk (FWHM= θ)	$I(\alpha,\beta)=\frac{1}{\sqrt{\pi/4\ln 2}\theta}\exp(\frac{-4\ln 2\rho^2}{\theta^2})$ (15) where $\rho=\sqrt{\alpha^2+\beta^2}$	$V(u,v)=\exp(-\frac{(\pi\theta\sqrt{u^2+v^2})^2}{4\ln 2})$ (16)	Basic representation of an enveloppe. Useful for a first order size estimation.
Uniform disk (diameter θ)	$I(\rho)=\begin{cases}4/(\pi\theta^2) & if\rho\leq\theta/2\\ 0 & if\rho>\theta/2\end{cases}$ (17)	$V(u,v)=2\frac{J_1(\pi\theta r)}{\pi\theta r}$ (18)	This model is the first order representation of a stellar surface with uniform intensisty distribution
Binary • (Flux, Position Star 1: F_1,α_1,β_1) • (Flux, Position Star 2: F_2,α_2,β_2)	$I(\alpha,\beta)=F_1\delta(\alpha-\alpha_1,\beta-\beta_1)+F_2\delta(\alpha-\alpha_2,\beta-\beta_2)$ (19)	$\lvert V(u,v)\rvert^2=\frac{1+f^2+2f\cos(2\pi/\lambda\vec{B}\vec{\rho})}{(1+f)^2}$ (20)	See section 3.2 for more details
Circular thin ring (radius ρ_0)	$I(\rho)=\frac{1}{2\pi\rho_0}\delta(\rho-\rho_0)$ (21)	$V(u,v)=J_0(2\pi\rho_0 r)$ (22)	

Table 1
Simple visibility building blocks

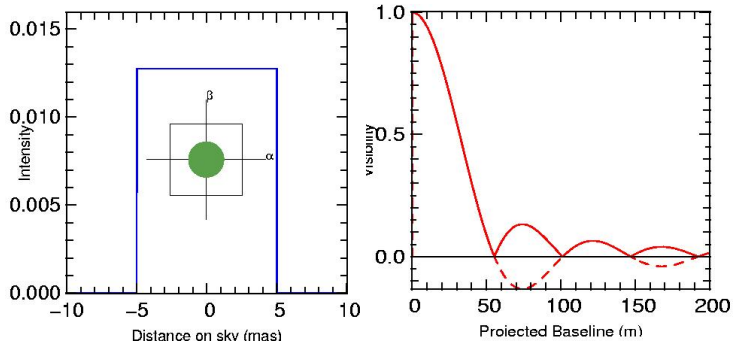

Fig. 2. Left: uniform disk model brightness distribution (θ = 10mas). The curve represents a cut across the brightness distribution. Right: Corresponding visibility curve as a function of baseline ($\lambda = 2.2\mu$m). The solid line is the visibility amplitude the dashed line the complex one. Four zeros and five lobes are visible. The sign inversion in the complex visibility curve implies a 180° phase shift.

2.4 Visibility building blocks

Initial observations with optical interferometers were limited to a small number of visibility points. Fitting strategy were therefore limited to "simple" but mostly unphysical models whose goal was mainly to provide first order (although precise) size and position angles estimations. These models are described in table 1.

2.4.1 Point source

Mainly used as description of unresolved objects with finite energy. When located at a distance from the pointing center (the one defined by the vector $\vec{s}$) the complex visibility includes a phase shift. The expected normalized visibility is 1 but when involved in the construction of a complex object its flux and phase should be taken into account. The phase has an obvious linear dependance with angular position on the sky.

2.4.2 Uniform disk

The uniform disk is the most simple model to describe the photospheric emission of a star (see Figure 2).

This is the first model to use when one wants to extract a diameter from a visibility curve. The visibility curve has several zeroes whose positions can be directly related with the diameter. If B_1 is the baseline corresponding to the first zero, then the diameter in milliarcseconds is $\theta = 251.6''\lambda/B_1$. Finding the

first zero is of course not mandatory, a χ^2 minimization on a properly sampled visibililty curve is the best way to get an accurate final result.

Note that Equation 18 shows that visibility changes sign as it goes through the zero. The observational consequence of this is that the interferogram phase shifts by 180°. Because phase is lost in the measurement process, this won't be directly observable but can be recovered by the measurement of closure phases (see J.D. Monnier same volume).

Any departure from the uniform disk model, caused for example by limb-darkening or brightening or the presence of a hot spot, should mostly affect spatial frequencies higher than the first null and therefore should require exploration of the second lobe. The reader is referred to the work by J. Young (same volume) for more details.

2.4.3 Gaussian disk

The Gaussian disk brightness distribution is often used to estimate the size of a resolved envelope with smooth limits.

2.4.4 Thin ring

The thin ring is the basic building block used to compute visibility curves of complex centro-symmetric objects. It is particularly useful when one is able to provide an analytical expression of radial intensity (e.g through a radiative transfer calculation.)

3 Constructing the visibility of a complex object

We will now see how to use those visibility building blocks in order to construct a more complex model. We will first show in section 3.1 how to modify a visibility function to take into account an inclination and position angle effect. Then we will see in section 3.2 how to construct the visibility curve out of the objects subelements visibilities.

3.1 Inclined or deformed structure.

It is often the case that inclination is one of the unknown parameters when modeling an object. Inclining with an angle i a circularly symmetric object can be seen as the effect of applying a $\cos(i)$ compression factor along one of its

axis (which becomes a semi-minor axis). The resulting structure displays an elliptical central symmetry. The addition of a new parameter, the semi-major axis orientation Θ (that we shall call position angle for convenience) is now required.

The link between the visibility curve of a circularly symmetric intensity distribution and its inclined and rotated version is obtained by a proper change in the baseline reference frame that takes into account a rotation:

$$\begin{cases} u_\Theta &= u\cos\Theta + v\sin\Theta \\ v_\Theta &= -u\sin\Theta + v\cos\Theta \end{cases} \tag{23}$$

followed by a compression factor $\cos(i)$ along the proper baseline axis.

In this new reference the elliptically symmetric object recovers a circular shape and standard visibility equations such as those described in table 1 can be used. In that new reference the projected baseline in units of wavelength $r_{uv\Theta i}$ can be written as:

$$r_{uv\Theta i} = \sqrt{u_\Theta^2 + v_\Theta^2\cos(i)^2} \tag{24}$$

As an example the visibility of a thin ellipse with semi-major axis ρ_0 can be computed from equation 10:

$$V(u,v) = J_0(2\pi\rho_0 r_{uv\Theta i}) \tag{25}$$

Another way to see this computation is considering that having an object smaller in one dimension with respect to its perpendicular due to an inclination is similar to observing a circularly symmetric object with a smaller baseline (less resolving power) in one direction with respect to its perpendicular.

3.2 A multicomponent object.

Let us consider now an astrophysical object that can be described by the addition of n components of known morphologies. Let us denote the brightness distributions of such objects $I_j(\alpha,\beta)$ their position in the plane of sky being (α_j,β_j) respectively and the corresponding normalized visibilities $V(u,v)$ with $j = 1..n$. To compute the normalized visibility of such an object one should take into account their respective contributions to the total brightness, which we will name F_j. The total brightness distribution can therefore be written:

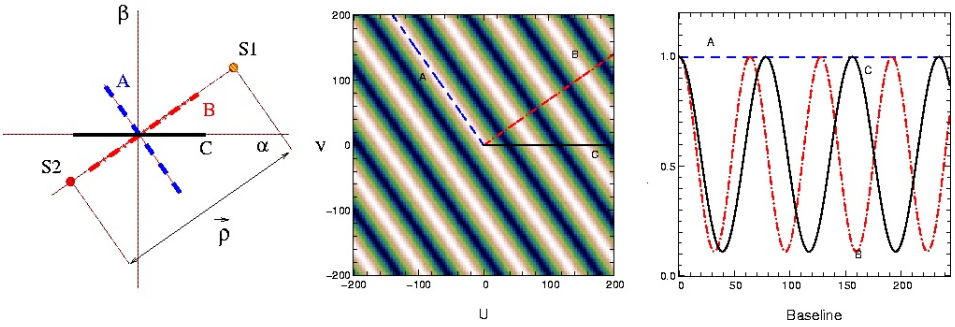

Fig. 3. Left: an unequal binary the plane of the sky. The binary separation ρ is 5 mas, the PA $\theta = 35°$, the flux ratio 0.5, and the wavelength of observation 1.55μm. The lines symbolizes three different baselines with different projected angles (dashed (A): 125°, dash-dotted (B): 35°, solid (C): 0°). Center: Image of the square of the visibility amplitude in the (u,v) plane obtained for such a binary. The lines show what part of the (u,v) is explored with the previous baselines. A maximum baseline of 200 m has been choosen here. Right: Corresponding square visibility curves corresponding to the three baselines (see text for comments).

$$I(\alpha, \beta) = \sum_{j=1..n} I_j(\alpha, \beta)\delta(\alpha - \alpha_j, \beta - \beta_j) \tag{26}$$

The addition property of the Fourier transform allows to write the visibility function as:

$$\nu(u, v) = \sum_{j=1..n} F_j V_j(u, v) \exp(2\pi i(u\alpha_j + v\beta_j)) \tag{27}$$

Normalization gives the final visibility:

$$V(u, v) = \frac{\sum_{j=1..n} F_j V(u, v) \exp(2\pi i(u\alpha_j + v\beta_j))}{\sum_{j=1..n} F_j} \tag{28}$$

3.3 The simplest complex object: the resolved binary

Binary star observations, together with diameter measurements, are the most widespread scientific observations made with interferometers so far. We can now use the same procedure as described in Section 3.2 to compute the visibility. The expression of the brightness distribution of a binary system (stars S_1 and S_2) with separation ρ, position angle θ and respective fluxes F_1 and F_2 is simply the sum of two unresolved point brightnesses (see Figure 3 and Equation 13).

$$I(\alpha,\beta) = F_1\delta(\alpha-\alpha_1,\beta-\beta_1) + F_2\delta(\alpha-\alpha_2,\beta-\beta_2) \tag{29}$$

where (α_1,β_1) and (α_2,β_2) are the angular coordinates for stars S_1 and S_2. The corresponding Fourier transform gives the unnormalized complex visibility function:

$$\nu(u,v) = F_1\exp(2\pi i(u\alpha_1+v\beta_1)) + F_2\exp(2\pi i(u\alpha_2+v\beta_2)) \tag{30}$$

The normalized squared visibility amplitude is then:

$$|V(u,v)|^2 = \frac{\nu(u,v)\nu(u,v)^*}{|\nu(0,0)|^2} \tag{31}$$

$$= \frac{F_1^2+F_2^2+2F_1F_2\cos(2\pi(u(\alpha_1-\alpha_2)+v(\beta_1-\beta_2)))}{(F_1+F_2)^2} \tag{32}$$

where the normalisation factor is the total flux squared ($\nu^2(0,0)$). If we introduce the flux ratio $f=\frac{F_2}{F_1}$ the baseline vector $\vec{B}$ ($|B| = \lambda\sqrt{u^2+v^2}$) and the separation vector $\vec{\rho}$ ($|\rho| = \sqrt{(\alpha_1-\alpha_2)^2+(\beta_1-\beta_2)^2}$) Equation 32 becomes:

$$|V(u,v)|^2 = \frac{1+f^2+2f\cos(2\pi/\lambda\vec{B}\vec{\rho})}{(1+f)^2} \tag{33}$$

Figure 3 shows a binary example ($|\vec{\rho}|$= 5 mas, the PA 35° and f=0.5). The corresponding squared visibility in the (u,v) plane is displayed in the center. It has a typical rippled structure. When looking at a squared visibility curve along three different projected baselines (at right in Figure 3) one can see very different responses [2]. Projected baseline A is perpendicular to the line linking the two components. Consider the analogy to the Young's Double Slit Experiment with two sources instead of one. If the projection of the line between the two sources along the optical axis [3] is perpendicular to the line between the two holes, then the optical path from one source to each of the two slits is the same. Therefore the fringe center for the two sources will be located at the same point in the screen whatever the distance between the slits. No visibility variation with slit separation is to be expected.

[2] These baseline coverages are of course unrealistic since earth rotation will induce elliptical tracks in the (u,v) plane

[3] The optical and pointing axis is defined for example as the line linking the center of the two sources to the center of the two slits.

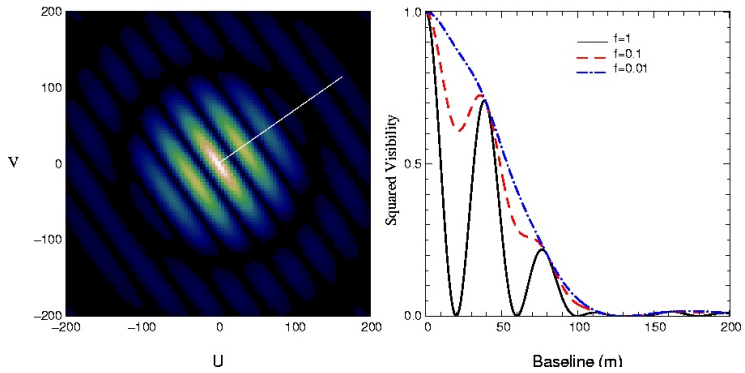

Fig. 4. Left: squared visibility in the (u, v) plane for a binary whose two stars have uniform disk diameters of 3 mas and are separated from each other by 8 mas (realistic ?) with a position angle 35° ($\lambda = 1.55\mu$m). The left side of the figure displays the squared visibility expected in the (u, v) plane when the flux ratio is one. The right side shows the squared visibility curves as a function of baseline (oriented at PA 35°) for three different flux ratios (solid, dash, dashdot curves respectively correspond to $f = 1, 0.1, 0.01$.

Two other baselines at two different angles will lead to two curves with different periods but the same amplitude. However it is most probable in practice that the earth rotation will lead to non linear cuts accross the (u, v) plane.

Now let us consider that both stars have finite size, i.e can be resolved by the interferometer. If $V_1(u, v)$ and $V_2(u, v)$ are the visibility curves for S_1 and S_2 stars respectively it is easy to write the expression of the visibility for the binary:

$$V(u,v) = \frac{V_1^2 + f^2 V_2^2 + 2f|V_1||V_2|\cos(2\pi/\lambda \vec{B}\vec{\rho})}{(1+f)^2} \tag{34}$$

Figure 4 shows the squared visibility as a function of baseline for a binary whose two stars are also resolved. The squared visibility curves appear as a modulation of the classical uniform disk shape by a cosine function caused by the binary. The amplitude of the modulation decreases when the flux ratio gets smaller. For a flux ratio of $f = 0.001$ the influence of the companion is barely noticeable.

In fact, Equation 34 can be used for any kind of structure involving two different components for which individual visibilities are known, for example a star+ envelope system.

4 A detailed example: an accretion disk

Accretion disks are important objects in astrophysics. They can be found in objects as different as young stars and active galactic nuclei. They are the bridge linking a surrounding diffuse medium with the compact central object (a star or a black-hole) and their physics, still poorly known is the subject of active research. Infrared interferometry has allowed to observe numerous disks around young stars with astronomical unit resolution. Analytical models of such objects have been proposed and are extremely useful for fast simulteneous spectral energy distribution and visibility fitting routines no narrow down the parameter space prior to more detailed modeling. We use what has been seen previously to describe here the visibility expression for such objects as a function of wavelength.

The derivation adopted her can undoubtely be adapted to any analytical model arising from radiative transfer computation.

4.1 The disk model

In its simplest version the image of an accretion disk can be seen as the continuous succession of thin circular rings with increasing radius (spanning from r_{min} to r_{max}) surrounding a central star. The temperature radial distribution of such as disk follows a power law:

$$T(r) = T_0(\frac{r}{r_0})^{-q} \tag{35}$$

where r_0 is a reference radius and T_0 is the temperature at this distance. The exponent q is the consequence of specific radiative transfer conditions and varies with the disk viscosity, flaring etc...

Each annulus is considered as a blackbody emitting at temperature $T(r)$. The total integrated flux received from an object located at distance d from the observer for a given wavelength is therefore the integration of all the rings contributions:

$$F_\lambda(0) = \frac{2\pi}{d^2}\int_{r_{min}}^{r_{max}} rB_\lambda(T(r))dr \tag{36}$$

for an inclined disk (angle i) the received flux becomes:

$$F_\lambda(i) = F_\lambda(0)\cos i \tag{37}$$

and the disk can be seen as the continuous succession of elliptical thin rings. The disk position angle is Θ.

4.2 Computing the visibility

The inclined accretion disk image is described as a sum (integral) of elliptical thin rings and therefore as we have seen in section 3.2 the corresponding visibility is just the sum (integral) of their Fourier transform weighted by their blackbody emission flux.

$$V_\lambda = \frac{1}{F_\lambda(0)} \int_{r_{min}}^{r_{max}} r B_\lambda(T(r)) J_0(2\pi r_{uv\Theta i} \frac{r}{d}) \, \mathrm{d}r \tag{38}$$

where

$$r_{uv\Theta i} = \sqrt{u_\theta^2 + v_\theta^2 \cos(i)^2} \tag{39}$$

represents the projected baseline in the a new (u_θ, v_θ) reference frame corresponding to the rotation of the array frame in the position angle Θ reference with a $\cos(i)$ compression factor.

The interested reader can see how this model has been succesfully applied to the peculiar case of Fu Orionis a young star observed with several interferometers (Malbet et al , 2005).

5 Conclusion and recommendations

Visibility (and closure phase) modeling still has a bright future. Even when second generation imaging instruments for Keck, Chara or MROI will be available the fourier space will remain the best place to quantify the intensity distribution through adjustment (fitting an image is hard). Moreover, it is most probably that preliminary inspection in the visibility space will probably help providing priors to be used by image reconstruction softwares.

A few obvious but worthwhile things remain to be recalled:

- the more complex the visibility model the more parameters will need to be fit and therefore the more datapoints are required;
- in the context of a limited amount of attributed time the observer will have to think carefully where in the spatial frequency space these datapoints

should be taken. This in order to get the best constraint on the parameters. For example, an observer interested in a diameter estimation will be wise to get a visibility measurement as closed as technically possible from the first zero. In the case of a binary the choice of points will have to be made so that the visibility oscillation amplitude is correctly sampled. *To summarize, while preparing his proposal the astronomer should already try to get a global picture of what can be expected in order to choose a pertinent telescope configuration capable of constraining the different sizes, orientations and flux ratios required.*

- If the object's angular size is too small to be resolved in the classical sense (object bigger than the beam size as defined by the ration of wavelength over the projected baseline) it is still possible to derive quantitative parameters from its visibility curve (exploiting the so-called "superresolution"). This is because modeling visibilities is a deconvolution process. However, one should remember that if components are barely resolved it will be hard to find out which is the best choice of model, since all the basic visibilities described earlier have quadratic dependencies toward small spatial frequencies (Lachaume 2003). The definition of "barely resolved" will of course depend on the accuracy with which the visibility measurements are made.
- The astronomer should be aware of the existence of different field of notions. The interferometer field of view (the one of interest in the visibility modelling process) is roughly λ/B. However, individual telescope arrays have also a limited field of view which is often caused by the presence of spatial filtering (fiber of pinhole) whose function is to improve visibility precision or simply because light is sampled by a single pixel. This field of view is roughly equal to the difraction limit of the telescope λ/D [4] if equipped with adaptive optics or atmospheric seeing if not λ/r_0 [5]. While computing its visibility model the astronomer should keep in mind the potential presence of a bias resulting from the presence of any emission source that is not in the interferometer field of view but contributes to the incoherent flux because it is in the field of view of the individual telescopes (e.g a companion and an envelope). This will result in an underestimation of the true visibility that can only be corrected by including the incoherent flux.
- A high visibility measured at one baseline, for example 99% can be modelled with a small extension but bright structure or a very extented envelope with a 1% contribution to the global flux. *The additional contribution of spectral energy distributions analysis or any other technique capable of constraining the different objects relative flux is essential for a good visibility fit.*

[4] D individual telescope diameter

[5] r_0: is the atmospheric fried parameter

References